Magnetism and magnetoresistance studies of $HfFe_6Ge_6$-type $Y_{1-x}Ce_xMn_6Sn_6$ (x = 0.1–0.3) compounds

2004 J. Phys.: Condens. Matter 16 147

(http://iopscience.iop.org/0953-8984/16/1/014)

INSTITUTE OF PHYSICS PUBLISHING JOURNAL OF PHYSICS: CONDENSED MATTER

J. Phys.: Condens. Matter **16** (2004) 147–154 PII: S0953-8984(04)69432-X

Magnetism and magnetoresistance studies of $HfFe_6Ge_6$-type $Y_{1-x}Ce_xMn_6Sn_6$ (x = 0.1–0.3) compounds

Jin-lei Yao[1,2], Shao-ying Zhang[1], Bao-dan Liu[1], De-ren Yang[2], Mi Yan[2], Ru-wu Wang[3], Li-gang Zhang[3] and Bao-gen Shen[1]

[1] State Key Laboratory of Magnetism, Institute of Physics and Centre for Condensed Matter Physics, Chinese Academy of Sciences, Beijing 100080, People's Republic of China
[2] State Key Laboratory of Silicon Materials, Zhejiang University, Hangzhou 310027, People's Republic of China
[3] Department of Applied Physics, University of Science and Technology of Wuhan, Wuhan 430081, People's Republic of China

E-mail: roger@g203.iphy.ac.cn (Jin-lei Yao)

Received 24 September 2003
Published 15 December 2003
Online at stacks.iop.org/JPhysCM/16/147 (DOI: 10.1088/0953-8984/16/1/014)

Abstract

Magnetic transitions and the magnetoresistance (MR) effect of the $HfFe_6Ge_6$-type $Y_{1-x}Ce_xMn_6Sn_6$ (x = 0.1–0.3) compounds have been investigated in the temperature range of 5–385 K. $Y_{0.9}Ce_{0.1}Mn_6Sn_6$ and $Y_{0.825}Ce_{0.175}Mn_6Sn_6$ show antiferromagnetism and $Y_{0.7}Ce_{0.3}Mn_6Sn_6$ undergoes an antiferromagnetic (AFM) to ferrimagnetic (Fi) transition with increasing temperature. The metamagnetic transition from helical antiferromagnetism to ferrimagnetism can be also induced by an applied field for those compounds. The metamagnetic transition field decreases with increasing Ce content, such as from 25 kOe for $x = 0.1$ to 11 kOe for $x = 0.3$ at 5 K. The giant MR (GMR) effect for $Y_{1-x}Ce_xMn_6Sn_6$ (x = 0.1–0.3) is observed with metamagnetic behaviour, such as -37% at 5 K under a field of 50 kOe for the compounds (x = 0.175 and 0.3). It is found that the MR behaviour for $Y_{0.7}Ce_{0.3}Mn_6Sn_6$ in the Fi state follows the magnetic-field power law MR $\propto -H^q$ at a fixed temperature, and obeys the relationship MR $= -[\alpha + \beta/(T + \gamma)]$ under a fixed magnetic field.

1. Introduction

Rare-earth manganese compounds of the RMn_6X_6 (R = rare earth, X = Sn, Ge) type have been reported to possess a rich variety of magnetic structures and interesting magnetic properties [1–10]. All these $HfFe_6Ge_6$-type (space group $P6/mmm$) RMn_6X_6 compounds are composed

of R and Mn layers alternately stacked along the c axis in the sequence Mn–(R, X)–Mn–X–X–X–Mn. The interlayer Mn–Mn coupling through the Mn–X–X–X–Mn slab is always ferromagnetic (FM) while that through the Mn–(R, X)–Mn slab depends on the nature of the R elements [2]. So, as naturally layered materials, RMn_6X_6 compounds provide an interesting complement to studies of artificial multilayer materials. Recently, the giant magnetoresistance (GMR) effect has been observed in derivatives of YMn_6Sn_6, i.e., $YMn_6Sn_{5.8}Ga_{0.2}$ [3], $Y_{0.5}Ho_{0.5}Mn_6Sn_6$ [4], and $YMn_6Sn_{5.9}In_{0.1}$ [5]. YMn_6Sn_6 shows an inhomogeneous helical antiferromagnetic (AFM) arrangement with Néel temperature $T_N = 333$ K [6], and undergoes a metamagnetic transition to the FM state at 20 kOe accompanied by a MR effect of -5% under a field of 50 kOe at 5 K [3]. The helical magnetic structure and the metamagnetic transition in YMn_6Sn_6 suggest that the exchange interactions between interlayers are weak and very sensitive to the nature of the R elements [6]. In this paper, we investigate the effects of Ce substitution for Y on the magnetic and transport properties of the $Y_{1-x}Ce_xMn_6Sn_6$ ($x = 0.1$–0.3) compounds.

2. Experiments

The $Y_{1-x}Ce_xMn_6Sn_6$ ($x = 0.1$–0.7) polycrystalline samples were synthesized by arc melting the constituent elements in a highly purified Ar atmosphere, and then annealing at 730 °C for ten days. X-ray diffraction (XRD) studies were carried out using a Rigaku Rint 1400 diffractometer with Cu Kα radiation at room temperature. The magnetization measurements for free-powder samples were carried out over the temperature interval of 5–385 K using a superconducting quantum interference device magnetometer with a maximum field of 50 kOe. The magnetoresistance (MR) measurements were carried out using the standard four-probe dc technique with an electric current (100 mA) parallel to the magnetic field. The samples used for the MR measurements were square cross-section rods in dimensions of $10 \times 2 \times 2$ mm^3.

3. Results and discussion

Although the structure of $CeMn_6Sn_6$ has not so far been identified [7], the samples ($x \leqslant 0.3$) display peaks characteristic of the $HfFe_6Ge_6$-type structure on their XRD patterns (see figure 1), and $Y_{1-x}Ce_xMn_6Sn_6$ ($x = 0.4$–0.7) crystallize to an unknown structure or are mixtures of multi-phases. As discussed by Venturini *et al*, the stability of the $HeFe_6Ge_6$-type structure for RMn_6Sn_6 compounds is related to the mean ionic radius (r_m) of the ions lying on the R site: $r_m \leqslant 0.094$ nm [8]. Assuming $r_{Y^{3+}} = 0.0893$ nm and $r_{Ce^{3+}} = 0.1034$ nm, the content of Ce in $Y_{1-x}Ce_xMn_6Sn_6$ whose structure is $HfFe_6Ge_6$-type should obey the relationship $x \leqslant 0.33$. The cell parameters of all the samples are gathered in table 1. Due to the larger ionic radius of Ce compared with that of Y, the substitution leads to an increase of the cell parameters a and c. However, the ratio c/a is constant for all the samples, indicating an isotropy expansion. The Mn–Mn interatomic distance in (001) Mn planes is equal to $a/2$, and that between layers is proportional to c. So the increase of the lattice constants by the substitution means the enlargement of the Mn–Mn interatomic distances within and between the layers.

The temperature dependence of the magnetization for $Y_{1-x}Ce_xMn_6Sn_6$ ($x = 0.1$–0.3) at 0.1 kOe after zero-field cooling is shown in figure 2(a). The $Y_{1-x}Ce_xMn_6Sn_6$ ($x \leqslant 0.175$) samples display AFM behaviour below T_N, while $Y_{0.7}Ce_{0.3}Mn_6Sn_6$ undergoes a magnetic transition from the AFM to the ferrimagnetic (Fi) state with increasing temperature. Since the introduction of small quantities of Ce in the YMn_6Sn_6 matrix does not greatly change the magnetic structure in the AFM state, $Y_{1-x}Ce_xMn_6Sn_6$ ($x = 0.1$–0.3) may be considered

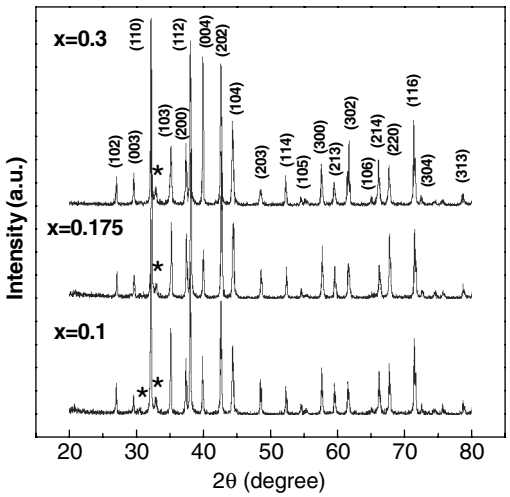

Figure 1. XRD patterns of $Y_{1-x}Ce_xMn_6Sn_6$ at room temperature. The asterisks indicate the peaks of an unknown impurity phase.

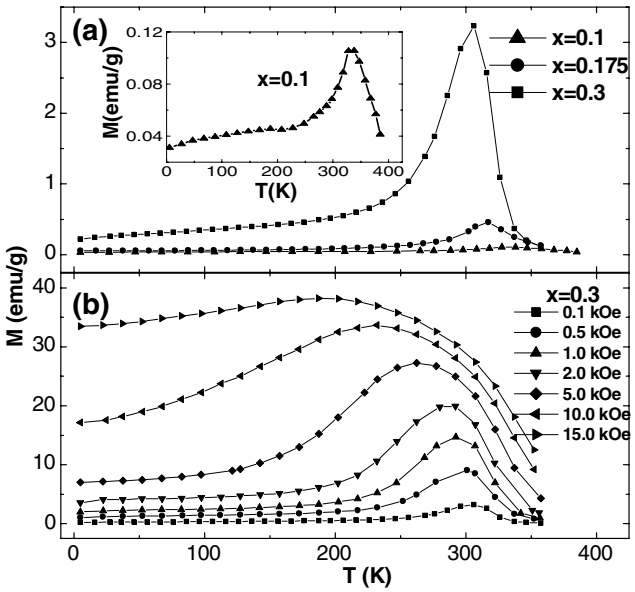

Figure 2. The temperature (T) dependence of magnetization (M) for $Y_{1-x}Ce_xMn_6Sn_6$ at 0.1 kOe (a), and for $Y_{0.7}Ce_{0.3}Mn_6Sn_6$ in various external magnetic fields (b). The inset shows the temperature dependence of magnetization for $x = 0.1$ in detail.

as possessing helical antiferromagnetism. The magnetic data are listed in table 1. To understand the effect of the external magnetic field on magnetic properties, we have measured the temperature dependence of the magnetization for $x = 0.3$ in various fields (see figure 2(b)). The strong influence of the magnetic field on magnetic properties is observed in the AFM state between 5 and 285 K, and the temperature range of the AFM state narrows with increasing magnetic field. The external magnetic field equal to 15 kOe can transform the sample into the Fi state, implying a metamagnetic transition.

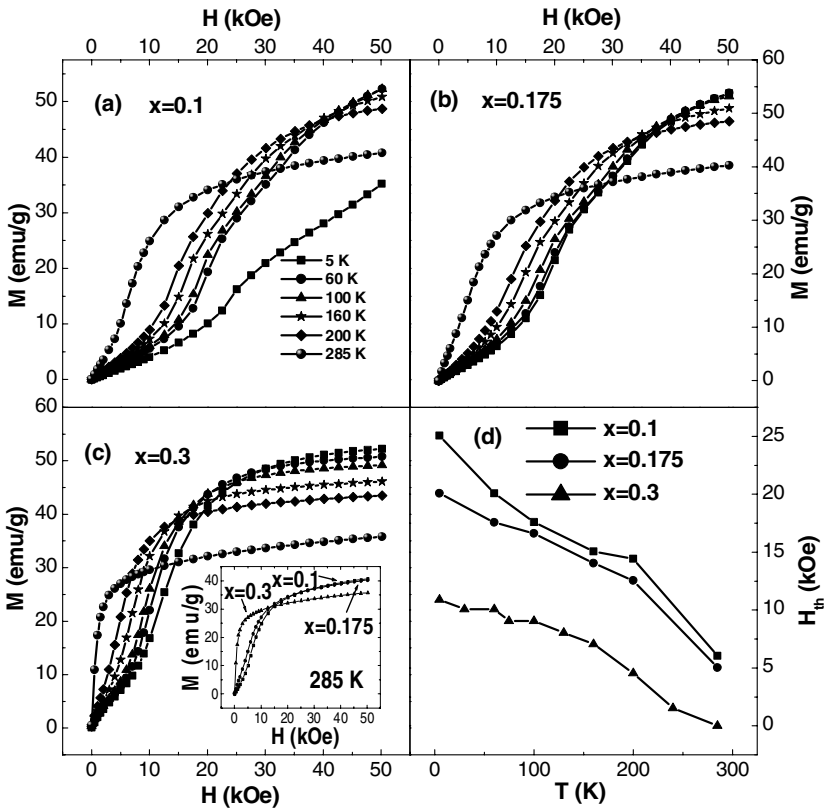

Figure 3. The magnetic field dependence of magnetization for $Y_{1-x}Ce_xMn_6Sn_6$ at various temperatures (a), (b), and (c); the thermal variation of the threshold field H_{th} for $Y_{1-x}Ce_xMn_6Sn_6$ (d). The inset shows the isothermal magnetization curves at 285 K for $x = 0.1$–0.3.

Table 1. Structural and magnetic data for the $Y_{1-x}Ce_xMn_6Sn_6$ compounds.

x	a (nm)	c (nm)	c/a	v (nm^3)	Type of magnetic ordering	$T_{C,N}$ (K)
0 [1]	0.5512	0.8984	1.630	0.2364	AFM	333
0.1	0.5531	0.9003	1.628	0.2385	AFM	328
0.175	0.5537	0.9016	1.628	0.2394	AFM	317
0.3	0.5543	0.9022	1.628	0.2401	AFM–Fi	316

Figure 3 shows the magnetic field dependence of the magnetization at various temperatures for the powder samples. For $Y_{1-x}Ce_xMn_6Sn_6$ ($x = 0.1$–0.3), the magnetization is proportional to the field in a low-field region and then shows a steep increase at a fixed temperature, indicating a metamagnetic transition from an AFM to an Fi state. The threshold field (H_{th}), taken at the maximum slope of the magnetization isotherms, decreases monotonically with increasing temperature. This is in good agreement with the results shown in figure 2(b). As shown in figure 3(d), H_{th} decreases markedly with increasing the content of Ce in $Y_{1-x}Ce_xMn_6Sn_6$ ($x = 0.1$–0.3), such as from 25 kOe for $x = 0.1$ to 10.9 kOe for $x = 0.3$ at 5 K. The significant decrease in H_{th} with increasing temperature and the content of Ce indirectly reflects the weakness of AFM characteristic for $Y_{1-x}Ce_xMn_6Sn_6$ ($x = 0.1$–0.3).

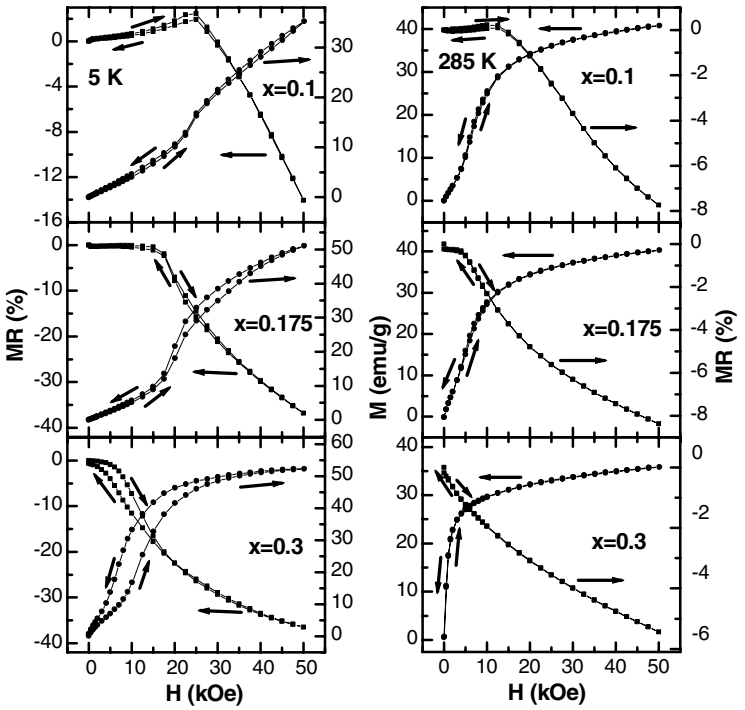

Figure 4. The magnetic field dependence of MR and magnetization for $Y_{1-x}Ce_xMn_6Sn_6$ at 5 and 285 K.

For cell parameters varying slightly (by less than 0.2%) by the introduction of small quantities of Ce, the interlayer Mn moments in $Y_{1-x}Ce_xMn_6Sn_6$ ($x = 0.1$–0.3) may be considered to be the same as in YMn_6Sn_6, rotating with a nonconstant angle [6]. The thermal and isothermal magnetization curves display unambiguously the AFM characteristic of $Y_{1-x}Ce_xMn_6Sn_6$ ($x \leqslant 0.175$) in their whole magnetic ordering range and of $x = 0.3$ at lower temperatures, in agreement with the results in the literature [8]. At higher temperatures, for example, at 285 K, the magnetization tends to saturation up to 50 kOe and decreases with increasing the content of Ce (see the inset of figure 3), suggesting that the magnetic moment of Ce is antiparallel to the magnetic moment of Mn. Moreover, according to neutron diffraction measurements on $Y_{0.8}Tb_{0.2}Mn_6Sn_6$, whose magnetic behaviour resembles that of $Y_{0.7}Ce_{0.3}Mn_6Sn_6$, it was shown that its magnetic structure is similar to that of YMn_6Sn_6 in the AFM state, and in the Fi state the magnetic moments of Mn are antiparallel to those of Tb and the moments have a small helical components on the c plane [9]. From the high-field studies on free powders of $RMn_{6-x}Cr_xSn_6$ ($x = 0$–3) in terms of the three-sublattice model, the threshold field of the transition from an AFM or collinear Fi configuration to a canted quasi-two-sublattice arrangement is of the order of 10 T, and the FM saturation of the compounds can be achieved in fields higher than 100 T [10]. So, as isostructural compounds, $Y_{1-x}Ce_xMn_6Sn_6$ ($x = 0.1$–0.3) should be of the Fi configuration rather than the FM or canted two-sublattice arrangement in the applied field range below 5 T. Summarily, it is reasonable to consider that $Y_{1-x}Ce_xMn_6Sn_6$ ($x \leqslant 0.175$) shows the helical AFM arrangement and $Y_{0.7}Ce_{0.3}Mn_6Sn_6$ undergoes the AFM to Fi transition with increasing temperature, and that sufficient magnetic field can switch the compounds from the AFM to Fi configuration. However, accurate studies

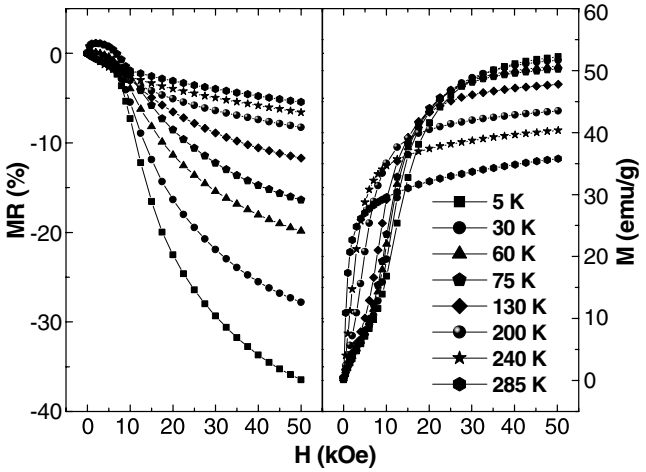

Figure 5. The magnetic field dependence of MR and magnetization for $Y_{0.7}Ce_{0.3}Mn_6Sn_6$ at various temperatures.

on the magnetic structures of $Y_{1-x}Ce_xMn_6Sn_6$ ($x = 0.1$–0.3), for example neutron diffraction and/or Mössbauer measurements, are required.

The temperature dependence of the resistance (R) for $x = 0.3$ was measured over the temperature interval of 5–370 K in zero and 50 kOe field. R follows a typical metallic behaviour. The ratio $[R(H) - R(0)]/R(0)$ is used to represent the MR. Figure 4 shows the field dependences of the MR and magnetization for $Y_{1-x}Ce_xMn_6Sn_6$ ($x = 0.1$–0.3) at 5 and 285 K, by first increasing the magnetic field to 50 kOe and then decreasing it to zero field. At 5 K, the sudden development of negative MR around H_{th} indicates that the samples undergo a metamagnetic transition from an AFM to Fi state. The GMR effect found in the samples might be related to spin-dependent electron scattering, as observed in artificial magnetic multilayers [11]. This transition is accompanied by the onset of marked hysteresis in the M–H and MR–H curves. Similar transitions in MR have earlier been observed in $SmMn_2Ge_2$-based compounds [12]. With the higher content of Ce, the metamagnetic transition can be achieved in the lower magnetic field in MR–H measurement, and the MR changes from -14% at $x = 0.1$ to -37% at $x = 0.3$ at 5 K. Similar phenomena have been also observed at 285 K. It is worth noting that no field hysteresis exists in MR–H and M–H curves for $x = 0.3$, which is related to $Y_{0.7}Ce_{0.3}Mn_6Sn_6$ going into the Fi state at 285 K. However, the MR for $x = 0.3$ still remains -5.4% at 50 kOe.

To better understand the thermal and magnetic field characteristics of the MR effect for the $Y_{1-x}Ce_xMn_6Sn_6$ ($x = 0.1$–0.3) series, we have measured the magnetic field dependence of the MR and magnetization for $x = 0.3$ at various temperatures (see figure 5). The MR increases as the temperature decreases due to the reduction of phonon scattering and spin-flip scattering by magnons [13]. However, no saturation in magnetization and MR is observed up to fields of 50 kOe.

It is well recognized that the GMR behaviour in metallic multilayers and manganese perovskites thin films can be expressed as a power-law magnetic-field dependence, MR $\propto -H^q$, where q is a constant at a fixed temperature. At 285 K, the magnetic field dependence of MR can be well scaled by the power law, and figure 6 shows a good linear relationship between $\log \mathrm{MR}^*$ and $\log H$ where $\mathrm{MR}^* = -\mathrm{MR}$. However, at other temperatures, only the MR behaviour in the high field can be described by this relationship. For $Y_{0.7}Ce_{0.3}Mn_6Sn_6$,

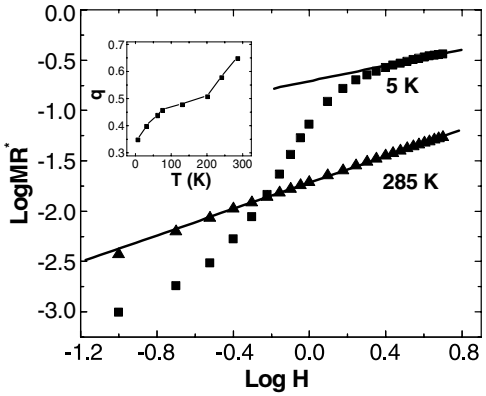

Figure 6. The relationship between log MR* (defined in text) and log H for $Y_{0.7}Ce_{0.3}Mn_6Sn_6$ at 5 and 285 K. Symbols represent the experimental data and solid lines denote the results scaled by the formulae $MR^* \propto H^q$. The inset shows the thermal variation of the exponent q.

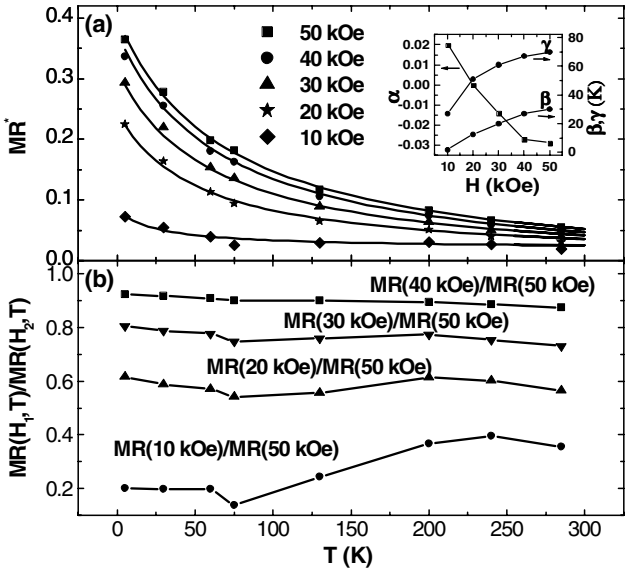

Figure 7. The temperature dependence of MR* (a) and $MR(H_1, T)/MR(H_2, T)$ (b) for $Y_{0.7}Ce_{0.3}Mn_6Sn_6$. The symbols represent the experimental data in various magnetic fields taken from the MR–H measurement (see figure 5), and the curves are fits of the form $MR^* = \alpha+\beta/(T+\gamma)$. The inset shows the magnetic field dependence of the parameters α, β, and γ.

it possesses the Fi configuration at 285 K and then it goes into the Fi arrangement when the external magnetic field exceeds the H_{th} below 285 K. So, for the $Y_{1-x}Ce_xMn_6Sn_6$ ($x = 0.1$–0.3) compounds, the magnetic-field power law is applicable only in the Fi state. The exponent q at various temperatures is shown in the inset of figure 6, and increases slightly with increasing temperature, indicating that q is a function of temperature.

Figure 7(a) shows the temperature dependence of MR* for $Y_{0.7}Ce_{0.3}Mn_6Sn_6$ in various magnetic fields. The MR* values (symbols in figure 7(a)) are taken from the MR–H curves in figure 5. Figure 7(b) shows the temperature dependence of the ratio of $MR(H_1, T)/MR(H_2, T)$, where H_1, H_2 represent the external magnetic fields. It is found

that the ratio $MR(H_1, T)/MR(H_2, T)$ where the magnetic fields exceed 15 kOe keeps almost constant between 5 and 285 K, with a deviation of about $\pm 7\%$. However, the curve of MR(10 kOe)/MR(50 kOe)–T fluctuates distinctly with increasing temperature. This suggests that the temperature dependence of MR in the Fi state can be determined totally as a field-independent function $G(T)$. For the $La_{2/3}Sr_{1/3}MnO_3$ polycrystalline samples, the thermal MR behaviour at low fields obeys the relationship $MR^* = \alpha + \beta/(T + \gamma)$ [14]. The temperature dependence of MR for $x = 0.3$ beyond 15 kOe can be also well scaled by the above formula. However, the MR values at 10 kOe slightly disobey this relationship as $Y_{0.7}Ce_{0.3}Mn_6Sn_6$ cannot totally go into the Fi state under a field of 10 kOe between 5 and 285 K (see figure 7(a)). The inset of figure 7(a) shows that the parameter α decreases monotonically with increasing magnetic field whereas the parameters β and γ possess weakly magnetic field dependence. As discussed by Hwang *et al* [14], this thermal MR effect for $La_{2/3}Sr_{1/3}MnO_3$ is associated with magnetic domain rotation at the grain boundaries. For $Y_{1-x}Ce_xMn_6Sn_6$ ($x = 0.1$–0.3), this effect can be attributed mainly to the transition of magnetic structures by the external magnetic field. The physical meaning of the MR effect for $Y_{1-x}Ce_xMn_6Sn_6$ ($x = 0.1$–0.3), however, is not completely clear at present. In addition, the relation of the magnetic structure and MR should be further studied.

4. Conclusions

In conclusion, we have examined the MR and magnetization for $Y_{1-x}Ce_xMn_6Sn_6$ ($x = 0.1$–0.3) between 5 and 385 K. With increasing the content of Ce, $Y_{1-x}Ce_xMn_6Sn_6$ ($x = 0.1$–0.3) show weaker AFM characteristics, and metamagnetic transitions can be induced by applying sufficiently strong magnetic fields. The threshold fields decrease almost monotonically with increasing temperature. Accompanying the metamagnetic transitions, the GMR effect is observed, such as for $x = 0.175$, $MR = -37\%$ at 5 K and, $MR = -8.4\%$ at 285 K under a field of 50 kOe, respectively. In the Fi state, the MR behaviour obeys the relationship of $MR(H, T) \propto F(H)G(T)$, where $F(H) = H^q$ and $G(T) = \alpha + \beta/(T + \gamma)$.

Acknowledgments

This work was supported by the State Key Project of Fundamental Research and National Natural Sciences Foundation of China.

References

[1] Malaman B, Venturini G and Roques B 1988 *Mater. Res. Bull.* **23** 1629
[2] Venturini G, Chafik El Idrissi B and Malaman B 1991 *J. Magn. Magn. Mater.* **94** 35
[3] Zhang S Y, Zhao P, Cheng Z H, Li R W, Sun J R, Zhang H W and Shen B G 2001 *Phys. Rev.* B **64** 212404
[4] Zhang S Y, Zhao T Y, Shen B G, Yao J L, Zhang L G, Li Y B and Li L 2002 *Appl. Phys. Lett.* **81** 3825
[5] Canepa F, Napoletano M, Lefevre C and Venturini G 2003 *J. Alloys Compounds* **349** 6
[6] Venturini G, Fruchart D and Malaman B 1996 *J. Alloys Compounds* **236** 102
[7] Weitzer F, Leithe-Jasper A, Hiebl K, Rogl P, Qi Q and Coey J M D 1993 *J. Appl. Phys.* **73** 8447
[8] Venturini G, Welter R and Malaman B 1993 *J. Alloys Compounds* **197** 101
[9] Shigeno Y, Kaneko K, Hori T, Iguchi Y, Yamaguchi Y, Sakon T and Motokawa M 2001 *J. Magn. Magn. Mater.* **226–230** 1153
[10] Brabers H V J, Zhou G F, Colpa J H P, Buschow K H J and de Boer F R 1994 *Physica* B **202** 1
[11] Baibich M N, Broto J M, Fert A, Nguyen Van Dau F, Petroff F, Etiene P, Creuzet G, Friederich A and Chazelas J 1988 *Phys. Rev. Lett.* **61** 2472
[12] van Dover R B, Gyorgy E M, Cava R J, Krajewski J J, Felder R J and Peck W F 1993 *Phys. Rev.* B **47** 6134
[13] Gijs M A M and Bauer G E W 1997 *Adv. Phys.* **40** 286
[14] Hwang H Y, Cheong S-W, Ong N P and Batlogg B 1996 *Phys. Rev. Lett.* **77** 2041